J Therm Anal Calorim (2011) 105:517–527
DOI 10.1007/s10973-010-1188-8

Compatibility study between ibuprofen and excipients in their physical mixtures

Bogdan Tiţa · Adriana Fuliaş · Zoltan Szabadai · Gerlinde Rusu · Geza Bandur · Dumitru Tiţa

ESTAC2010 Conference Special Issue

Abstract The thermal techniques of analysis were used to assess the compatibility between ibuprofen (IB) and some excipients used in the development of extended released formulations. This study is a part of a systematic study undertaken to find and optimizes a general method of detecting the drug–excipient interactions, with the aim of predicting rapidly and assuring the long-term stability of pharmaceutical product and speeding up its marketing. The thermal properties of IB and its physical association as binary mixtures with some common excipients were evaluated by thermogravimetry/derivative thermogravimetry (TG/DTG) and differential scanning calorimetry. FT-IR spectroscopy and X-ray powder diffraction (XRPD) were used as complementary techniques to adequately implement and assist in interpretation of the thermal results. Based on their frequent use in preformulations nine different excipients: starch; microcrystalline cellulose (PH 101 and PH 102); colloidal silicon dioxide; lactose (monohydrate and anhydre); polyvinylpyrrolidone; magnesium stearate and talc were blended with IB. The samples were prepared by mixing the analyte and excipients in a proportion of 1:1 (w:w). The TG/DSC curves of the IB have shown a single stage of mass loss between 175 and 290 °C, respectively, an endothermic peak at 78.5 °C, which corresponds to the melting (literature T_m = 75–78 °C).

Keywords Ibuprofen · Thermal behaviour · TG/DSC · Drug–excipient compatibility

B. Tiţa (✉) · A. Fuliaş · Z. Szabadai · D. Tiţa
Faculty of Pharmacy, University of Medicine and Pharmacy "Victor Babeş", Eftimie Murgu Square 2, 300041 Timişoara, Romania
e-mail: bogdantita@yahoo.com

G. Rusu · G. Bandur
Industrial Chemistry and Environmental Engineering Faculty, Politehnica University of Timişoara, Victoriei Square 2, 300006 Timişoara, Romania

Introduction

It is well known that the majority of anti-inflammatory drugs are carboxylic acids.

Ibuprofen, α-methyl-4-(2-methylpropyl)benzeneacetic acid, which structural formula is shown in Fig. 1, is a non-steroidal anti-inflammatory drug (NSAID), which exhibits favourable anti-inflammatory, analgesic and antipyretic properties.

The major clinical application on NSAIDs is their action as anti-inflammatory agents in muscle skeleton diseases [1]. The anti-inflammatory activity of NSAIDs and most of its other pharmacological effects are related to the inhibition of the conversion of arachidonic acid to prostaglandins, which are mediators of the inflammatory process [2, 3].

Ibuprofen is a potent inhibitor of cyclooxygenase (Cox) in vitro and in vivo, thereby decreasing the synthesis of prostaglandins, prostacyclin and thromboxane products.

Two different cyclooxygenase isoforms have been characterized, Cox-1 and Cox-2. Inhibition of the Cox-2 enzyme system results in anti-inflammatory action, whilst inhibition of the Cox-1 enzyme system results in anti-inflammatory action as well as gastric irritation. Consequently, research efforts have been directed towards evolving compounds which are specific Cox-2 inhibitors [4].

New studies from the past years revealed that in addition to arthritis and pain, cancer and neuro-degenerative

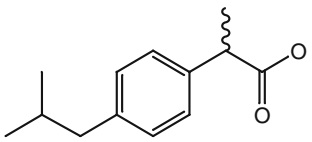

Fig. 1 The chemical structure of the IB

diseases like Alzheimer's disease could potentially be treated with Cox-2 inhibitors [5].

Studies of drug–excipient compatibility represent an important phase in the preformulation stage for the development of all dosage forms. In fact potential physical and chemical interactions between drugs and excipients can affect the chemical nature, the stability and bioavailability of drugs and, consequently, their therapeutic efficacy and safety.

Thermal analysis (TA) is a rapid analytical technique commonly used for evaluating drug–excipient interactions through the appearance, shift or disappearance of endo- or exothermal effects and/or variations in the relevant enthalpy values [6–11].

In our previous articles [12–16] we provided the importance of the thermal and kinetic analysis in estimation on the thermal behaviour of different pharmaceuticals.

However, the interpretation of the thermal data is not always easy and, to avoid misinterpretations and misleading of TA results, it must be emphasized that the interactions observed at high temperatures may not always be relevant under ambient conditions. Moreover, the presence of a solid–solid interaction does not necessarily indicate pharmaceutical incompatibility, but it might instead be advantageous, e.g. as a more desirable form of drug delivery system [17–22]. Therefore, the use of other analytical techniques, such as infrared spectroscopy, X-ray powder diffractometry and hot-stage microscopy as complementary tools to assist in the interpretation of TA findings, is greatly advisable [23–25].

In a previous study [26], a study regarding the thermal stability and kinetic analysis of ibuprofen (IB) under non-isothermal conditions was realized.

The purpose of this article is to evaluate the compatibility of IB with common pharmaceutical excipients, used in the solid dosage form, by TA, Fourier transformed infrared (FT-IR) and X-ray powder diffraction patterns (XRPD).

Experimental

Materials and samples

The IB drug and the excipients: starch; microcrystalline cellulose PH 101 (MC-101) and PH 102 (MC-102); colloidal silicon dioxide (CSD); lactose monohydrate (α-lactose); lactose anhydre (β-lactose); polyvinylpyrrolidone K30 (PVP K30 or PVP); magnesium stearate (MS) and talc were obtained from Terapia S.A./Ranbaxy, Cluj-Napoca, Roumania as pure compounds, able to be used for medical purpose.

Physical mixtures of IB with each selected excipient were prepared in the 1:1 (*w:w*) ratio by simple mixture of the components in an agate mortar with pestle for approximately 5 min.

Methods

Thermal analysis

The TG/DTG curves were recorded using a Netzsch-STA 449 TG/DTA instrument in the temperature range 20–500 °C, under a dynamic atmosphere of nitrogen (20 mL min^{-1}) and at a heating rate (β) of 10 °C min^{-1}, using platinum crucibles and weighed approximately 20 mg of samples.

DSC experiments were carried out with a Netzsch differential scanning calorimeter, model DSC-204, using aluminium crucibles with approximately 3 mg of samples, under dynamic nitrogen atmosphere (50 mL min^{-1}) and a heating rate of 10 °C min^{-1}, up to a temperature of 500 °C.

Fourier transformed infrared spectroscopy (FT-IR) and X-ray diffraction

FT-IR spectra of drug, excipients and drug–excipients blends were recorded on a Perkin–Elmer Model 1600 apparatus using KBr discs in the range 4000–400 cm^{-1}.

X-ray powder diffraction patterns were obtained with a Bruker D8 Advance X-ray diffractometer using MoK_α radiation (Zr filter on the diffracted beam, 50 kV and 40 mA) in a Bragg–Brentano θ:2θ configuration, with Soller and fixed slits and a NaI (Tl) scintillation detector. The measurements of 2θ ranged between 0° and 30°. Data analysis and acquisition were performed using DIFFRACT^{plus} software from Bruker AXS.

Results and discussion

The thermoanalytical curves of IB are presented in Fig. 2.

The TG/DTG curves show that IB is stable up to 175 °C and presents a single stage of mass loss between 175 and 290 °C ($\Delta m = 98\%$) and $DTG_{peak} = 282.5$ °C.

The DSC curve has shown a sharp endothermic peak ($T_{peak} = 78.5$ °C; $T_{onset} = 72.4$ °C; $\Delta H_{fus} = -448$ J g^{-1}) corresponding to the melting point, followed by other endothermic peak due to decomposition ($T_{peak} = 271$ °C).

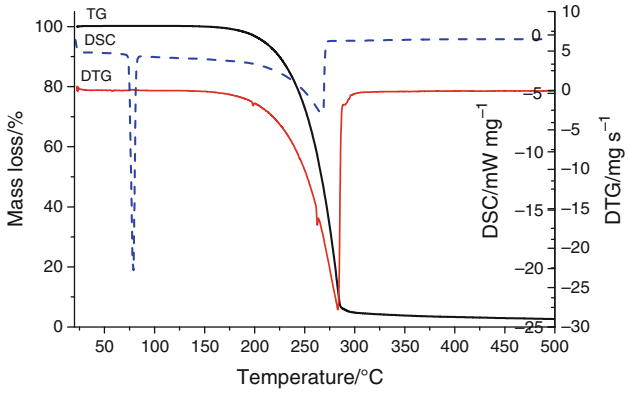

Fig. 2 TG/DTG and DSC curves of IB

Compatibility study with excipients

Figures 3, 4 and 5 show the TG, DTG and DSC curves of the substances used in the compatibility study.

The TG/DTG curves of starch show a dehydration between 33 and 120 °C ($\Delta m = 7.2\%$; $DTG_{peak} = 65$ °C), followed by the process of decomposition between 295 and 375 °C ($DTG_{peak} = 325$ °C; $\Delta m = 79.7\%$). Initially the DSC curve exhibits a wide endothermic peak representing dehydration ($T_{peak} = 94$ °C) [6, 17, 27].

The thermal behaviour of microcrystalline cellulose PH 101 and PH 102 is the same. Absorbed water (about 5%) is lost below 110 °C, between 35 and 110 °C, apparently in a single, endothermic and spread-out process ($DSC_{peak} = 72$ °C). No other thermal phenomena are observed before the beginning of decomposition, between 307 and 385 °C ($DTG_{peak} = 355$ °C and $\Delta m = 88\%$), respectively, $DSC_{peak} = 320$ °C [21, 22, 27, 28].

In the case of the CSD, on the thermoanalytical curves, no peak was observed in the range 25–500 °C [18, 22, 27].

The amorphous form of lactose was identified by the presence of an exothermic peak at 167 °C, which represented the transformation of amorphous to crystalline form. It is followed by two endothermic peaks, one at 210 and the other at 216 °C. These melting peaks belong to α- and β-lactose, respectively. It confirmed the transformation of the amorphous form of lactose to the two types of crystalline form by heating [29–31].

The 100% crystalline lactose, according to XRPD, contains α and β forms.

According to the thermogram, the water-content ($\Delta m = 4.5\%$) of α-lactose monohydrate is evolved between 100 and 170 °C ($DTG_{peak} = 161$ °C). The water-free compound is stable up to about 265 °C, then it decomposes up to 365 °C and $DTG_{peak} = 315$ °C. The DSC curve shows a first sharp endothermic peak ($T_{peak} = 145$ °C) corresponding to the dehydration reaction, followed by two endothermic peaks, from the first sharp endothermic peak ($DSC_{peak} = 215$ °C), which corresponds to the melting of α-lactose, the second weak peak ($DSC_{peak} = 224$ °C) represents the melting of β-lactose [22, 27, 30, 31].

On the DSC curve, the β-lactose presents a small endothermic peak ($T_{peak} = 145$ °C) with an insignificant mass loss on the TG curve, followed by two peaks, the first light corresponds to the melting of α-lactose ($T_{peak} = 215$ °C), respectively, the second represents the melting of the β-lactose ($T_{peak} = 224$ °C). The decomposition process takes place in the temperature range 275–365 °C ($DTG_{peak} = 312$ °C), accompanied by an endothermic event on the DSC curve ($T_{peak} = 318$ °C) [22, 27, 32, 33].

The TG/DSC curves of PVP, below 150 °C, display an initial mass loss of ≈9%. This mass loss is accompanied by a broad endothermic phenomena ($DSC_{peak} = 82$ °C) over an ill-defined baseline which makes evaluation of the dehydration enthalpy quite uncertain. The sample readily dehydrates and its initial mass depends upon the moisture content of the atmosphere. Apparently, dehydration is completed at 110 °C ($DTG_{peak} = 164$ °C) in N_2. However, a second loss stage (≈2%) begins past 150 °C and

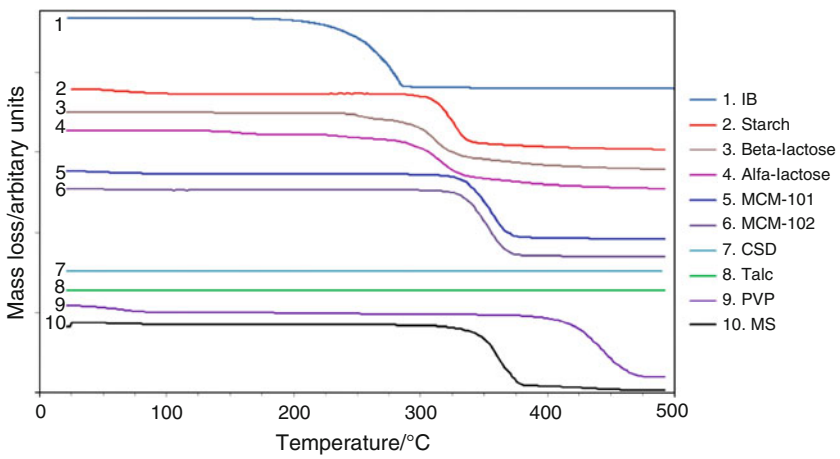

Fig. 3 TG curves of all substances used in compatibility study

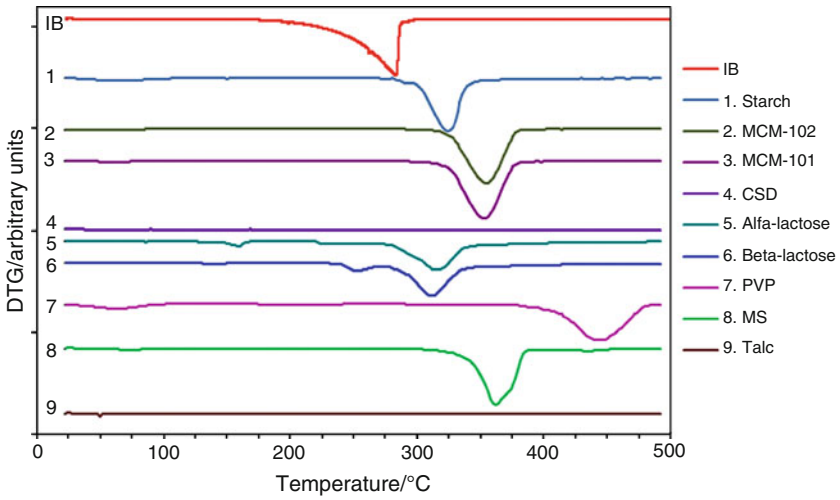

Fig. 4 DTG curves of all substances used in compatibility study

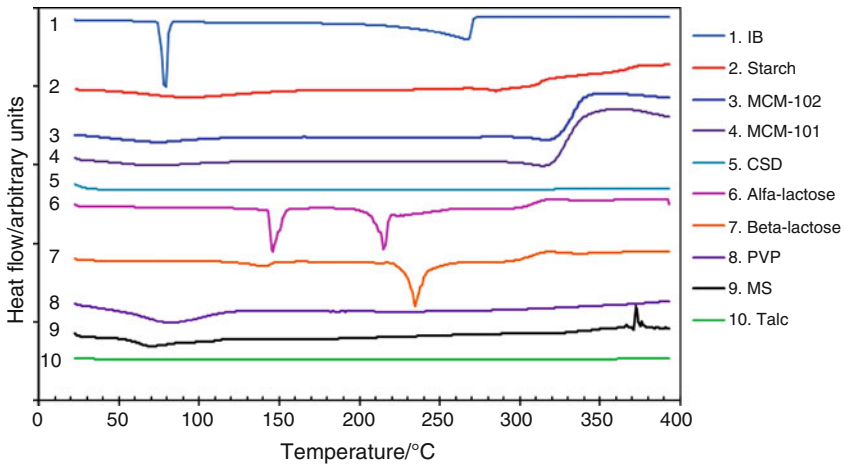

Fig. 5 DSC curves of all substances used in compatibility study

completes around 250 °C. TA, SEM and XRPD all show that the compound is in a vitreous phase with glass transition near 200 °C. Decomposition begins around 384 °C (DTG_{peak} = 442 °C, Δm = 86%) up to 485 °C [21, 28, 34–36].

Simultaneous TG/DSC curves of MS show several dehydration stages below 110 °C. The first endothermic effect is due to release of a small amount of surface water. Around 50 °C begins the first dehydration stage of structural water, which partially overlaps with a second stage at higher temperature. The overall mass loss due to surface water and to the first stage is ≈3%, whilst the amplitude of the second stage is ≈1.5% of the initial mass. DSC curve of MS initially shows wide endothermic effect (T_{peak} = 75 °C), representing dehydration. Melting begins at ≈110 °C and produces an endothermic peak with a shoulder in the high temperature side which is caused by melting of magnesium palmitate or high-melting polymorphs. The decomposition of the sample begins around 311 °C (DTG_{peak} = 362 °C) and at 480 °C, 92.5% of sample mass is lost. Corresponding to the decomposition process, the DSC curve presents a sharp endothermic peak with T_{max} = 372 °C [21, 27, 28, 32, 33, 36].

The TG/DTG and DSC curves of talc present any significant events under the conditions in this study [22, 27, 32, 33, 36].

TG, DTG and DSC curves of the pure IB and the 1:1 drug:excipient physical mixture are shown in Figs. 6, 7 and 8.

In the 1:1 physical mixtures when there is no interaction between drug and excipient the T_{peak} value of melting event (DSC curve) and the first stage of the decomposition (T_{onset} and T_{peak} of TG/DTG curves) should remain practically unchanged, similarly when the drug is alone. In this case the thermal profiles of the mixture can be considered as a superposition of the curves of the IB and excipients. In the DSC curve the T_{peak} value of melting of the drug is alone, or in its mixtures when there is no interaction between drug and excipient.

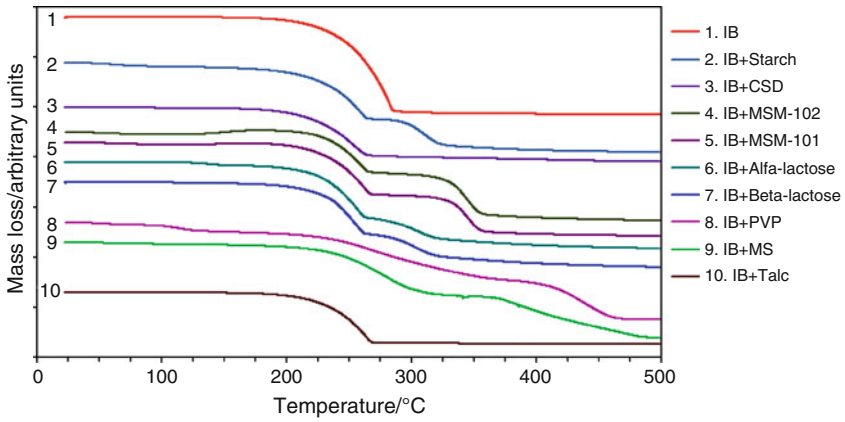

Fig. 6 TG curves of IB and its 1:1 physical mixtures

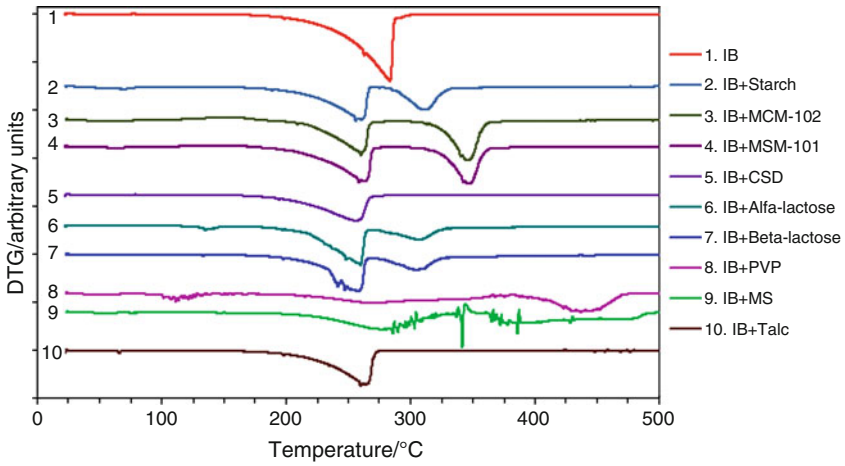

Fig. 7 DTG curves of IB and its 1:1 physical mixtures

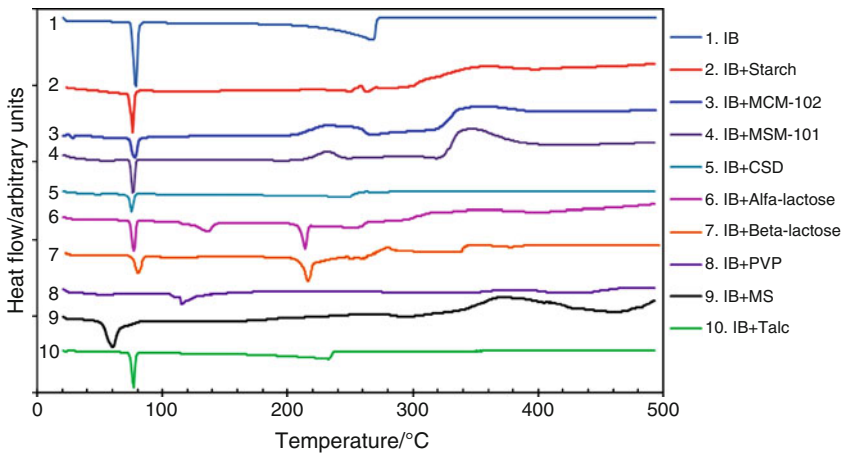

Fig. 8 DSC curves of IB and its 1:1 physical mixtures

According to the thermal curves (Figs. 6, 7, 8), especially DSC curves that provide the most complete information, it is found some smaller or larger differences (the case of the mixtures with PVP and MS) in terms of the melting temperature values and those of the thermal decomposition ranges. Basically, all the other excipients present some differences, however small, on the melting temperature, respectively, the value of the melting enthalpies (Table 1). These differences may be due to the small interactions that have not been confirmed by FT-IR spectroscopy and XRPD.

In the case of mixtures with povidone (PVP) and MS, the DSC curves demonstrated differences in the thermal profile of the IB, such as absence of drug's melting event.

Table 1 Thermoanalytical data of IB and drug:excipient physical mixtures

Samples	DSC		ΔH_{fusion}/J g^{-1}	$T_{peak\ DTG}$/°C	Δm/%
	$T_{onset\ (fusion)}$/°C	$T_{peak\ (fusion)}$/°C			
Drug					
IB	72.4	78.5	448	282	99
Drug/excipient					
Starch	71.1	77.1	198.8	255	5; 55; 30
MC-102	71.2	77.7	172	259	1; 41; 48
MC-101	71.3	76.5	188.2	258	1; 54; 40
CSD	66.9	76	109.7	253	55
α-lactose	71.0	77.1	185.3	259	3; 55; 32
β-lactose	72.3	77.5	159.1	256	2; 51; 32
PVP[a]				266	10; 50; 35
MS	50.0	58.8	336.6[b]	285	5; 53; 38
Talc	70.5	76.8	183.9	259	50

[a] The value not calculated due to absence of drug's melting event or undefined peak

[b] The value represents the sum of two or more processes not only drug's melting event

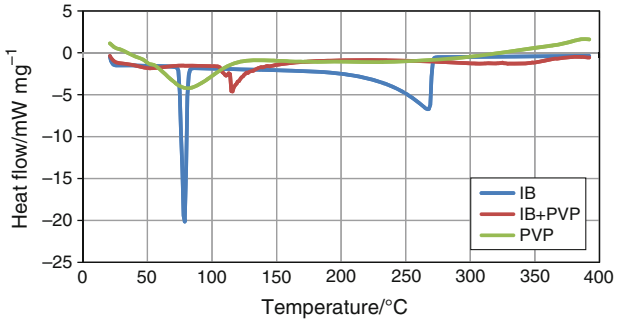

Fig. 9 DSC curves of IB, PVP and its 1:1 physical mixtures

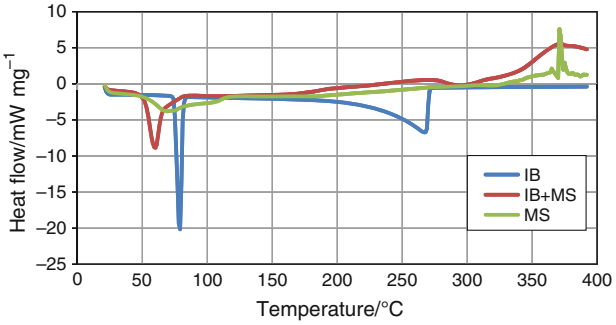

Fig. 10 DSC curves of IB, MS and its 1:1 physical mixtures

The TG curves demonstrated that excipients influence the decomposition process of the IB by displacing the T_{onset}, respectively, DTG_{peak} of the first mass loss event at a lower temperature than the isolated drug. Frequently, this displacing is due to structural change and indicates interaction, incompatibilities between the compounds.

The DSC curve of the physical mixture of IB with PVP demonstrated the disappearance of the characteristic IB fusion peak. Initially, the curve presents a broad and weak peak which corresponds to the elimination of the adsorbed water, between 40 and 95 °C with DSC_{peak} = 51.6 °C. This event is followed by a sharp peak with a shoulder on the left side which corresponds to the dehydration process of PVP, between 95 and 150 °C (DSC_{peak} = 115.4 °C) (Fig. 9).

The PVP interaction with IB takes place by so-called dissolution of IB in the presence of humidity. This process is met in the speciality literature for the cases of other drugs too (naproxen, captopril and cetoprofen) [21, 27, 28, 36–38].

For the IB mixture with MS, the DSC curves (Fig. 10) show the disappearance of the melting peak of IB ($T_{peak\ fusion}$ = 78.5 °C) and a new one appears at 20 °C below. Also, the decomposition intervals are wider. These differences are attributed to the interaction between the two components as happens in the case of MS' interaction with other drugs [6, 17, 22, 28, 34].

The results taken from the TG and DSC curves for the binary mixtures are collected in Table 1.

Decreasing values of ΔH_{fus} suggest that the process (in this case melting) takes place with low intensity or even disappears (the case of IB with povidone mixture for which ΔH_{fus} was not calculated).

Unlike the small differences of the melting temperatures, the values of ΔH_{fus} even less than half of the value corresponding to the IB show the possibility of interactions, especially for the CSD and β-lactose.

The FT-IR spectroscopy was used as a supplementary technique in order to investigate the possible chemical interaction between drug and excipient and to confirm the

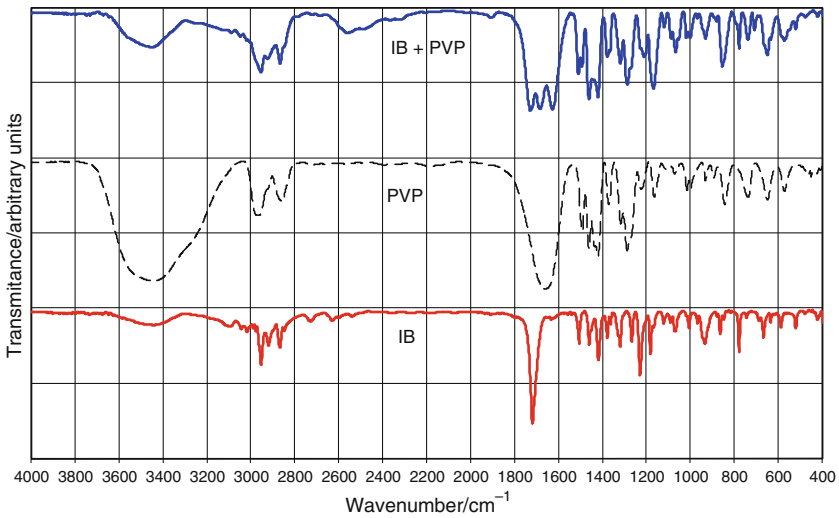

Fig. 11 IR spectra of PVP, IB and 1:1 blend as simple mixture of IB and PVP

results obtained by the TA. It is the most suitable technique of the non-destructive spectroscopic methods and has become an attractive method in the analysis of pharmaceutical solids, since the materials are not subject to thermal or mechanical energy during sample preparation, therefore, preventing solid-state transformations. The appearances of new absorption band(s), broadening of band(s), and alteration in intensity are the main characteristics to evidence interactions between drug and excipients [22, 27, 32, 39–41].

FT-IR spectra were drawn for IB, excipients, respectively, for the corresponding mixtures. Further, it will be presented only the spectra for the cases where the TA indicates a possible interaction, namely: IB, povidone and the mixture IB:povidone (Fig. 11), respectively, IB, MS and the corresponding mixture (Fig. 12).

For the other mixtures, the FT-IR spectra can be considered as the superposition of the individual ones without absence, shift or broadening in the vibration bands of IB. It demonstrated the absence of chemical interactions between IB and the corresponding excipients.

The IB spectrum was in accordance with the literature, which describes in the region of 3500 cm^{-1} a large attributed to the OH group present in the IB molecule (carboxyl group). In the region of 2977–2866 cm^{-1} there are three bands that correspond to the methylene and methyl group. The most intense band appears at 1742 cm^{-1} and represents the carbonyl vibration band. The methine group has a characteristic band in the 1338 cm^{-1} region, and the methylene group in the 1462 cm^{-1} region. The region of 1422–1241 cm^{-1} showed bands which correspond to the methyl symmetric C–H bending (δ_s CH_3), respectively, to the C–O stretching from carboxyl group. The band at 780 cm^{-1} corresponds to the out-of-plane C–H bending from phenyl ring.

In respect of the povidone, it presents the bands at:

- 3460 cm^{-1}—a large band attributed to the OH group from the crystallization water;
- 2977 cm^{-1}—that corresponds to the C = O binding;
- 1669 cm^{-1}—that corresponds to the carbonyl amidic group;
- 1495; 1465; 1422 cm^{-1}—these correspond to asymmetrical vibration (δ_{as} CH_3);
- 1291 cm^{-1}—that corresponds to the in-plane C–H bending.

For the binary mixture, it shows the following differences:

- The disappearance of the bands at 2738, respectively at 2636 cm^{-1} from the IB′ spectrum;
- The appearance of a broad band between 2572 and 2500 cm^{-1};
- It appears a triplet at 1733, 1692, 1633 cm^{-1} instead of the bands from 1721 cm^{-1} (IB) and 1669 cm^{-1} (PVP);

The FT-IR spectrum for the physical mixture between IB and PVP suggests some chemical interactions.

Magnesium stearate presents a strong ethyl vibration in the region of 2921 up to 2850 cm^{-1}. In the 1569–1468 cm^{-1} region, it showed an asymmetric stretch corresponding to the carboxyl anion.

Other bands that must be maintained have their peaks at 2958 cm^{-1} corresponding to asymmetric vibration of C–H bond in methyl group, respectively, those at 721 cm^{-1} which corresponds to "rocking" deformation $(H–C–H)_n$ $n > 3$.

FT-IR spectrum of IB–MS mixture shows the following changes:

- The band at 3461 cm^{-1} is more intense and less broad;

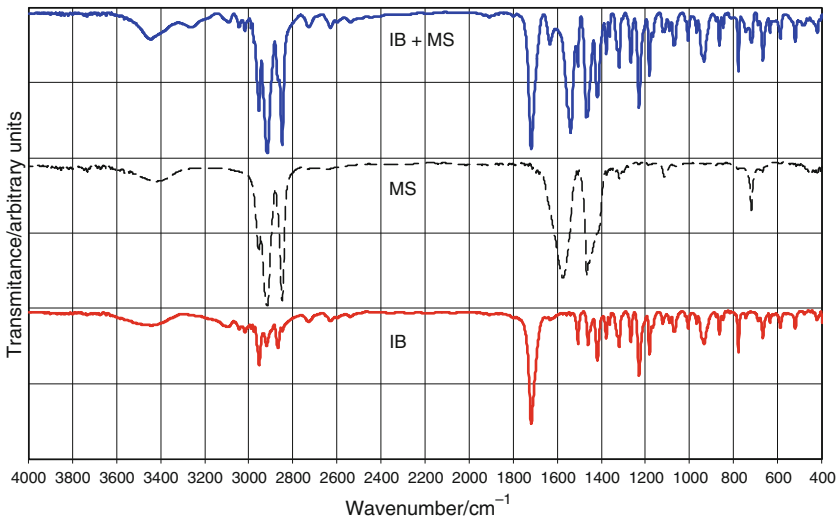

Fig. 12 IR spectra of MS, IB and 1:1 blend as simple mixture of IB and MS

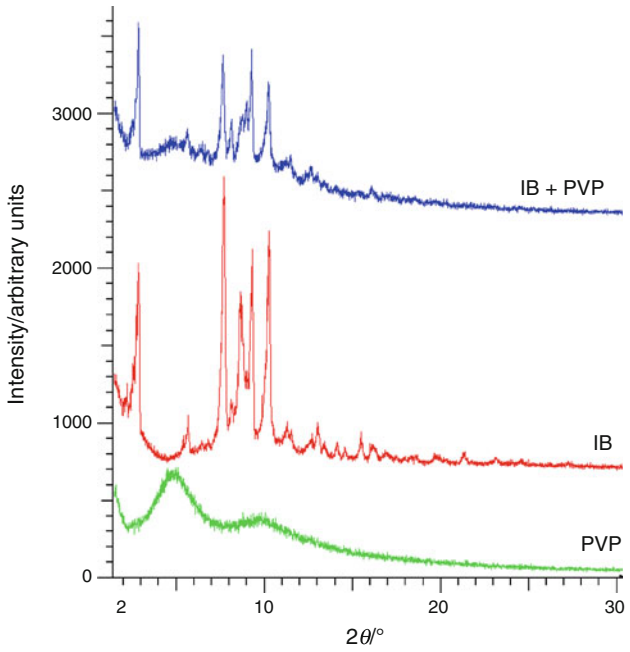

Fig. 13 X-ray diffractogram of PVP, IB and 1:1 blend as simple mixture of IB and PVP

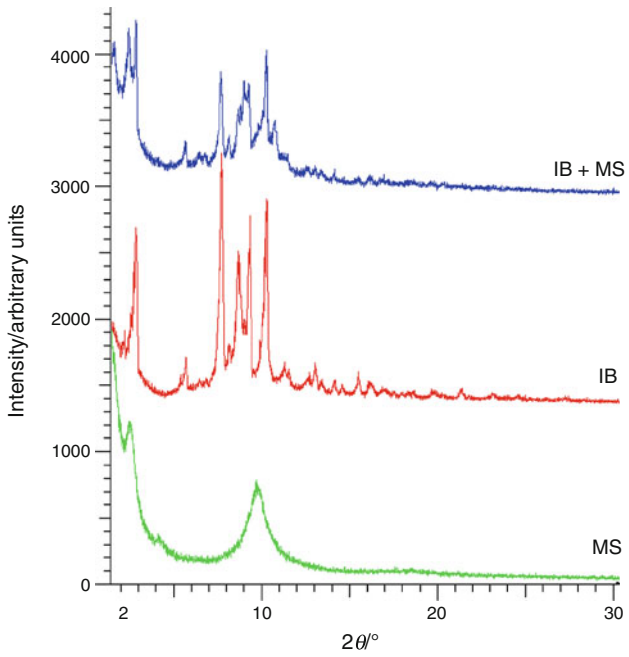

Fig. 14 X-ray diffractogram of MS, IB and 1:1 blend as simple mixture of IB and MS

- A new band appears at 3284 cm^{-1}, not very intense;
- The band at 1721 cm^{-1} is more intense (≈20%);
- A new band appears at 1638 cm^{-1}, relatively intense;
- The bands at 1380 and 1269 cm^{-1} are more intense (≈15–20%);
- The bands at 938, 780 and 669 cm^{-1} are more intense (≈10–15%).

From the above observations obtained after comparing the spectra, it may be considered that MS interacts with IB.

To investigate the possible interaction of IB with povidone and MS, besides the FT-IR spectroscopy which is a qualitative analysis technique, the X-ray powder diffraction has been used for qualitative and quantitative identification of crystallinity. The number of the speciality articles which uses the X-ray powder diffraction is growing [29, 31, 34, 35, 38, 41].

The XRPD of IB, povidone and IB–povidone mixture, respectively, IB, MS and IB–MS mixtures are shown in Figs. 13 and 14.

The additional proeminent DSC peaks in the mixtures of the drugs and excipients are a positive indication of chemical interaction of the drugs with excipients. Such interaction should result in the partial or complete disappearance of the reactant phases and appearance of new

Table 2 X-ray diffraction data for IB, povidone and IB–povidone (1:1) mixture

IB		IB7		7	
2θ	I%	2θ	I%	2θ	I%
2.156	27.7				
2.553	37.3				
2.812	71.6	2.799	100		
				4.824	100
5.648	17.3	5.603	47.6		
6.437	10.6	6.412	39.2		
6.802	11.1				
7.685	100	7.633	83.9		
8.119	24.7	8.108	52		
8.628	60.5	8.733	55.4		
8.975	34.5	8.958	61		
9.295	68.8	9.256	82.4		
				9.717	55.2
10.255	80.2	10.225	72		
11.29	16.3				
11.521	14.5	11.473	33.1		
12.708	11.5	12.639	27.8		
13.033	15.8	13.015	23.3		
13.397	9.9	13.398	20.1		
14.127	10.2				
14.589	8.3				
15.508	12.3				
16.199	9.4	16.106	16.6		

phases, which can be inferred from XRPD. XRPD of the mixture, prepared at room temperature, when compared with those of its individual components showed appearance of new lines and disappearance of some of the lines present in the individual components.

The X-ray patterns of IB–povidone mixture prepared at room temperature did not show the lines in addition to those present in patterns of the individual components (Table 2). However, the number of lines present in the XRD patterns of the individual components was found missing in the similar pattern recorded for the mixture. The significant difference in the X-ray patterns of the drug–excipient mixtures compared to those of individual drugs and excipient indicates possible incompatibility of the drugs with the excipient, even at room temperature. The presence of majority of the lines of the parent substances in the thoroughly ground mixture prepared at room temperature, however, suggests the interaction of the drug with the excipient at room temperature, which could increase with the increased temperature.

The number of new lines appeared in IB–MS mixture is shown in Table 3. The same table indicates disappearance

Table 3 X-ray diffraction data for IB, MS and IB–MS (1:1) mixture

IB		IB8		8	
2θ	I%	2θ	I%	2θ	I%
2,156	27.7				
		2.401	96		
				2.459	100
2,553	37.3				
2,812	71.6	2.81	100		
				4.095	27.6
5,648	17.3	5.627	30.7		
6,437	10.6	6.423	24.9		
		6.722	24.3		
6,802	11.1				
7,685	100	7.65	69.6		
8,119	24.7	8.111	34.6		
8,628	60.5	8.623	49		
		8.769	51.2		
8,975	34.5	8.969	63.4		
9,295	68.8	9.232	63.8		
				9.725	60.2
		10.043	48.4		
10,255	80.2	10.227	78.9		
		10.729	43.1		
11,29	16.3				
		11.466	23.5		
11,521	14.5				
12,708	11.5	12.642	17		
13,033	15.8	13.04	16.5		
13,397	9.9	13.355	14.8		
14,127	10.2	14.094	13.1		
14,589	8.3				
15,508	12.3				
16,199	9.4	16.088	11.4		
		16.695	10.4		

of some of the diffraction lines of higher, moderate and lower intensities in the mixture which are originally present in the XRPD of the individual components, which indicates the interaction of IB with MS.

Conclusions

This article presents an issue of great importance, met more and more often in the speciality literature: the compatibility of the drugs with different excipients.

The study refers to the compatibility of the IB with a range of excipients mentioned in the article. As methods of study, the following were used: the thermal methods of analysis, the FT-IR spectroscopy and XRPD.

According to the thermal curves, especially DSC curves, one can say that all excipients present lower or higher interactions, with IB. This fact is supported by the differences between the values of T_{top} and of the enthalpies of melting.

Considering that the enthalpies of melting are quantitative data since they may be expressed as a fractional change, it could be said that PVP and MS certainly interact with IB. In the same context, the CSD and β-lactose interaction occurs in a certain extent, whilst other excipients' interaction is unlikely.

The interaction of PVP and MS with IB was confirmed by FT-IR spectroscopy and by XRPD. In terms of β-lactose and CSD interaction with IB, this was not confirmed by the two techniques mentioned, probably because of limited modifications.

This study shows the incompatibility of IB with PVP and MS.

References

1. Kovala-Demertzi D. Recent advances on non-steroidal anti-inflammatory drugs, NSAIDs: Organotin complexes of NSAIDs. J Organomet Chem. 2006;691:1767–74.
2. Kafarska K, Czakis-Sulikowska D, Wolf WM. Novel Co(II) and Cd(II) complexes with non-steroidal anti-inflammatory drugs. Synthesis, properties and thermal investigation. J Therm Anal Calorim. 2009;96:617–21.
3. Teslyuk OI, Beltyukova SV, Yegorova AV, Yagodkin BN. Complex compounds of terbium(III) with some nonsteroidal anti-inflammatory drugs and their analytical applications. J Anal Chem. 2007;62:330–5.
4. Ying YC, Yi L, Cheng ZJ, Dan Z. Inhibitory effect of copper complex of indomethacin on bacteria studied by microcalorimetry. Biol Trace Elem Res. 2008;122:82–8.
5. Fini A, Fasio G, Benetti L, Ghedini V. Thermal analysis of some diclofenac salts with alkyl and alkylhydroxy amines. Thermochim Acta. 2007;464:65–74.
6. Mora Corvi P, Cirri M, Mura P. Differential scanning calorimetry as a screening technique in compatibility studies of DHEA extended release formulations. J Pharm Biomed Anal. 2006;42:3–10.
7. Neto HS, Barros FAP, de Sousa Carvalho FM, Matos JR, Thermal analysis of prednicarbate and characterization of thermal decomposition product, J Therm Anal Calorim. 2010. doi: 10.1007/s10973-009-0419-3.
8. Macêdo RO, Aragão CFS, do Nascimento TG, Macêdo AMC. Application of thermogravimetry in the quality control of chloramphenicol tablets. J Therm Anal Calorim. 1999;56:1323–7.
9. Moura EA, Correia LP, Pinto MF, Procopio JVV, de Sousa FS, Macedo RO. Thermal characterization of the solid state and raw material fluconazole by thermal analysis and pyrolysis coupled to GC/MS. J Therm Anal Calorim. 2010. doi:10.1007/s10973-009-0473-X.
10. Giordano F, Rossi A, Pasquali I, Bettini R, Frigo E, Gazzaniga A, Sangalli ME, Miles V, Catinella S. Thermal degradation and melting point determination of diclofenac. J Therm Anal Calorim. 2003;73:509–18.
11. Picciochi R, Diogo HP, da Piedade MEM. Thermochemistry of paracetamol. J Therm Anal Calorim. 2010;99:391–401.
12. Tiţa B, Marian E, Tiţa D, Vlase G, Doca N, Vlase T. Comparative kinetic study of decomposition of some diazepine derivatives under isothermal and non-isothermal conditions. J Therm Anal Calorim. 2008;94:447–52.
13. Tiţa B, Fuliaş A, Marian E, Tiţa D. Thermal behaviour of acetylsalicylic acid—active substance and tablets. Kinetic study under non-isothermal conditions. Rev Chim (Bucureşti). 2009;60:419–23.
14. Tiţa B, Fuliaş A, Marian E, Tiţa D. Thermal stability and decomposition kinetics under non-isothermal conditions of sodium diclofenac. Rev Chim (Bucureşti). 2009;60:524–8.
15. Fuliaş A, Tiţa B, Bandur G, Tiţa D. Thermal decomposition of some benzodiazepines under non-isothermal conditions. Kinetic study. Rev Chim (Bucureşti). 2009;60:1079–83.
16. Tiţa B, Fuliaş A, Rusu G, Tiţa D. Thermal behaviour of indomethacin—active substance and tablets kinetic study under non-isothermal conditions. Rev Chim (Bucureşti). 2009;60:1210–5.
17. Bernardi LS, Oliveira PR, Murakami FS, Silva MAS, Borgmann SHM, Cardoso SG. Characterization of venlafoxine with pharmaceutical excipients. J Therm Anal Calorim. 2009;97:729–33.
18. Moyano MA, Broussalis AM, Segall AI. Thermal analysis of lipoic acid and evaluation of the compatibility with excipients. J Therm Anal Calorim. 2010. doi:10.1007/s10973-009-0351-6.
19. Oliveira PR, Bernardi LS, Murakami FS, Mendes C, Silva MAS. Thermal characterization and compatibility studies of norfloxacin for development of extended release tablets. J Therm Anal Calorim. 2009;97:741–5.
20. Lira AM, Araújo AAS, Basílio IDJ, Santos BLL, Santana DP, Macedo RO. Compatibility studies of lapachol with pharmaceutical excipients for the development of topical formulations. Thermochim Acta. 2007;457:1–6.
21. Tomassetti M, Catalani A, Rossi V, Vecchio S. Thermal analysis study of the interactions between acetaminophen and excipients in solid dosage forms and in some binary mixtures. J Pharm Biomed Anal. 2005;37:949–55.
22. Barboza F, Vecchia DD, Tagliari MP, Silva MAS, Stulzer HK. Differential scanning calorimetry as a screening technique in compatibility studies of acyclovir extended release formulations. Pharm Chem J. 2009;43:363–8.
23. Bannach G, Cervini P, Cavalheiro ETG, Ionashiro M. Using thermal and spectroscopic data to investigate the thermal behaviour of drugs and excipients by unique calculations. J Therm Anal Calorim. 2010. doi:10.007/s10973-009-0595-1.
24. Iliescu T, Baia M, Miclăuş V. A Raman spectroscopic study of the diclofenac sodium-β-cyclodextrin interaction. Eur J Pharm Sci. 2004;22:487–95.
25. Bannach G, Cervini P, Cavalheiro ETG, Ionashiro M. Using thermal and spectroscopic data to investigate the thermal behaviour of drugs and excipients by unique calculations. Thermochim Acta. 2010;499:123–7.
26. Tiţa B, Fuliaş A, Bandur G, Rusu G, Tiţa D. Thermal stability of ibuprofen. Kinetic study under non-isothermal conditions. Rev Roum Chim. 2010;55:553–8.
27. Bertol CD, Cruz AP, Stulzer HK, Murakami FS, Silva MAS. Thermal decomposition kinetics and compatibility studies of primaquine under isothermal and non-isothermal conditions. J Therm Anal Calorim. 2010;102:187–92.
28. Marini A, Berbenni V, Moioli S, Bruni G, Cofrancesco P, Margheritis C. Drug–excipient compatibility studies by physico-chemical techniques. The case of indomethacin. J Therm Anal Calorim. 2003;73:529–45.
29. Gombas A, Szabo-Revesz P, Kata M, Regdon G Jr, Eros I. Quantitative determination of crystallinity of α-lactose monohydrate by DSC. J Therm Anal Calorim. 2002;68:503–10.
30. Balestrieri F, Magri AD, Magri AL, Marini D, Sacchini A. Application of differential scanning calorimetry to the study of

drug–excipient compatibility. Thermochim Acta. 1996;285:337–45.
31. Desai SR, Shaikh MM, Dharwadkar SR. Preformulation compatibility studies of etamsylate and fluconazole drugs with lactose by DSC. J Therm Anal Calorim. 2003;71:651–8.
32. Cides LCS, Araújo AAS, Santos-Filho M, Matos JR. Thermal behaviour, compatibility study and decomposition kinetics of glimepiride under isothermal and non-isothermal conditions. J Therm Anal Calorim. 2006;84:441–5.
33. Oliveira GGG, Ferraz HG, Matos JSR. Thermoanalytical study of glibenclamide and excipients. J Therm Anal Calorim. 2005;79:267–70.
34. Marini A, Berbenni V, Pegoretti M, Bruni G, Cofrancesco P, Sinistri C, Villa M. Drug–excipient compatibility studies by physico-chemical techniques. The case of atenolol. J Therm Anal Calorim. 2003;73:547–61.
35. Bruni G, Amici L, Berbenni V, Marini A, Orlandi A. Drug–excipient compatibility studies. J Therm Anal Calorim. 2002;68:561–73.
36. Nunes RS, Semaan FS, Riga AT, Cavalheiro ÉTG. Thermal behavior of verapamil hydrochloride and its association with excipients. J Therm Anal Calorim. 2009;97:349–53.
37. Stulzer HK, Tagliari MP, Cruz AP, Silva MAS, Laranjeira MCM. Compatibility studies between piroxicam and pharmaceutical excipients used in solid dosage forms. Pharm Chem J. 2008;42:215–9.
38. Stulzer HK, Rodrigues PO, Cardoso TM, Matos JSR, Silva MAS. Compatibility studies between captopril and pharmaceutical excipients used in tablets formulations. J Therm Anal Calorim. 2008;91:323–8.
39. Neto HS, Novák Cs, Matos JR. Thermal analysis and compatibility studies of prednicarbate with excipients used in semi solid pharmaceutical form. J Therm Anal Calorim. 2009;97:367–74.
40. Freire FD, Aragao CFS, e Moura TFA, Raffin FN. Compatibility study between chlorpropamide and excipients in their physical mixtures. J Therm Anal Calorim. 2009;97:355–7.
41. Abbas D, Kaloustian J, Orneto C, Piccerelle P, Portugal H, Nicolay A. DSC and physico-chemical properties of a substituted pyridoquinoline and its interaction study with excipients. J Therm Anal Calorim. 2008;93:353–60.